Environment International 202 (2025) 109587

Contents lists available at ScienceDirect

Environment International

journal homepage: www.elsevier.com/locate/envint

Full length article

New insights into car tire rubber particle toxicity: chemical composition and ecotoxicity assessment of leachate on gamete quality of the Mediterranean mussel *Mytilus galloprovincialis*

Ilaria Savino [a], Amir Nobahar [b], José P. Da Silva [b], Pietro Cotugno [c], Rosaria Notariale [d], Giuseppe Corriero [e], Vito Felice Uricchio [a], Alessandra Gallo [d,*]

[a] *Water Research Institute, Italian National Council of Research, CNR-IRSA, V.le F. De Blasio 5, 70132 Bari, Italy*
[b] *Centre of Marine Sciences (CCMAR/CIMAR LA), University of Algarve, Campus de Gambelas, 8005-139 Faro, Portugal*
[c] *Chemistry Department, University of Bari "Aldo Moro", Via Orabona 4, I-70126 Bari, Italy*
[d] *Department of Biology and Evolution of Marine Organisms, Stazione Zoologica Anton Dohrn, Villa Comunale 1, 80121 Naples, Italy*
[e] *Department of Biosciences, Biotechnologies and Environment, University of Bari Aldo Moro, 70125 Bari, Italy*

ARTICLE INFO

Handling Editor: Adrian Covaci

Keywords:
Bivalve mollusc
End-of-life car tire particle
Gamete quality assessment
Seawater leachate
Microplastic

ABSTRACT

Thousands of tire rubber particles (TPs) enter the marine environment every year, contributing to microplastic pollution. The toxicity of TPs can be related to the particles themselves or chemical additives, which can leach into seawater and potentially affect marine organisms. The current study presents new insights into TPs' impact on marine organisms' reproductive processes. The leachates of end-of-life TPs and their adverse effects on gamete quality were evaluated by analysing the chemical compositions of seawater leachates and several gamete physiological parameters, taking the mussel *Mytilus galloprovincialis* as a model. Chemical analyses revealed the leaching of different metals, among which zinc showed the highest level (~3 mg/L). Organic compounds such as antioxidants, vulcanising and protective agents were annotated in leachates and correlated with the observed harmful effects on the reproductive process. The exposure of oocytes and spermatozoa to TP leachates negatively affects the gamete quality by increasing the mitochondrial activity in both gamete types and decreasing the motility of spermatozoa, which may impair the reproductive success of mussels. Since reproductive success is a key factor in species survival, this study highlights the urgent need to extend the presented research to other marine organisms.

1. Introduction

Modern vehicle tires are typically composed of natural and synthetic rubber, such as styrene-butadiene rubber (SBR), a plastic copolymer possessing many other chemical additives (Xaydarali, 2022). Tire abrasion generated by friction between tires and roads during driving leads to breakdown into tiny plastic particles, which can be widespread in the surrounding environment, polluting air, water, and soil. The particles released from tires are considered one of the major sources of microplastics entering marine environments (Arole et al., 2023), primarily through road runoff, where rain washes them from roads into rivers and oceans. They can also be released directly from vehicles near coastal areas, through improper waste disposal, or from industrial activities. Additionally, small particles may pass through wastewater treatment systems and enter the ocean. Due to the extensive traffic rate in developed countries, microplastic emission through tire abrasion is a far-reaching problem (Gieré and Dietze, 2022). Other potential sources of tire wear particles are recycled tire crumb and tire repair-polished debris, which can also reach marine environments through wind and rain.

Currently, the assessment of tire wear particle toxicity is still a challenge. Tire wear particle toxicity should be based not only on the micrometer-sized particles themselves, but also on their chemical additives, degradation products, and contaminants adsorbed on their surface (Lv et al., 2024). Indeed, besides containing different proportions of natural and synthetic rubber, vehicle tires also include several different materials, such as silica and carbon black as fillers, oil and resin as softeners, zinc oxide and stearic acid as vulcanizing agents,

* Corresponding author.
E-mail address: alessandra.gallo@szn.it (A. Gallo).

https://doi.org/10.1016/j.envint.2025.109587
Received 8 July 2024; Received in revised form 12 May 2025; Accepted 3 June 2025
Available online 13 June 2025

along with several additives including preservatives, antioxidants, desiccants, plasticizers and processing aids (Xaydarali, 2022). As these compounds interact with rubber polymers by non-covalent bonds, they can readily leach into seawater and induce various biological responses in marine biota, being of major environmental concern (Li et al., 2023). Therefore, it is necessary to explore not only the toxic effects of rubber microparticles produced during tire wear but also the adverse effects of leached chemical additives on marine organisms. Different toxic effects of chemical compounds used in tire production on marine organisms have already been documented (Wik and Dave, 2009); however, further research is needed to comprehensively understand the potential toxicity of the complex chemical mixture leaching from tires in marine invertebrates. To date, harmful effects from tire wear particle leachates are reported in a few marine organisms, namely marine bacteria, macro and microalgae, copepods, sea urchins and mussels (Halsband et al., 2020; Rist et al., 2023; Tallec et al., 2022a; Turner and Rice, 2010). In particular, in the Mediterranean mussel *Mytilus galloprovincialis,* the potential effects of car tire rubber leachates were assessed on the fertilizing ability of spermatozoa and embryo development (Capolupo et al., 2020). However, their impact on oocyte quality is still unknown. Oocytes and spermatozoa are highly specialized cells generated in the gonad through gametogenesis, and their fusion marks the creation of a new individual. Thereby, the quality of male and female gametes is essential for successful fertilization and embryo development, influencing the fitness and well-being of the offspring (Romdhani et al., 2024b).

Commonly, in marine organisms, investigations into the quality of spermatozoa after exposure to various contaminants have focused solely on the fertilization rate as the endpoint, neglecting many other sperm quality parameters (Gallo et al., 2011; Gallo and Tosti, 2013, 2015; Warnau et al., 1996). On the other hand, although oocyte quality is also a crucial factor in fertilization and embryo development, the impact of contaminants on female gamete quality is seldom investigated (Esposito et al., 2024; Esposito et al., 2023; Tallec et al., 2022b). Our previous studies paved the way for assessing several physiological parameters in both male and female marine invertebrate gametes (Boni et al., 2022). These parameters are useful markers of healthy gametes representing valuable tools to investigate the toxicity and mechanism of action of marine contaminants within the framework of reproductive risk assessment (Gallo et al., 2016; Gallo et al., 2022; Gallo et al., 2021; Romdhani et al., 2024a).

The present study investigated the impact of the leachate generated in seawater from end-of-life vehicle tire particles on the quality of male and female gametes of the Mediterranean mussel *M. galloprovincialis* by evaluating different physiological parameters, including viability, mitochondrial activity, intracellular pH, and reactive oxygen species (ROS) levels. By assessing these parameters along with the chemical analysis of leachates, this study explores the threat posed by the complex chemical mixture leached by rubber tires on the quality of male and female mussel gametes, aiming to unveil the underlying toxic action mechanisms and correlate their chemical signatures with the observed toxicity.

2. Material and methods

2.1. Tire particles and leachate preparation

The tire particles (TPs) used in the present study were obtained from a local waste tire-crushing factory.

The end-of-life vehicle tires were mechanically shredded into granulated particles ranging from 0 to 0.8 mm in size. Then, the material was passed through a sieve with a specified pore size to isolate the particles smaller than 100 μm. These particles were then used to prepare the leachate. Based on previous studies (Capolupo et al., 2020; Halsband et al., 2020; Tallec et al., 2022b; Yang et al., 2022), 50 g of these particles were added to 1 L of filtered natural seawater (FNSW) in glass tubes. This mixture was stirred at 300 rpm at 18 °C for ten days in the dark. Afterwards, the mixture was filtered through a 0.22 μm filter membrane, and the tire particle leachate (TPL) was collected in a glass tube. Before storage at 4 °C, the pH and osmolarity of TPL were checked using a bench pH meter and an optical refractometer, respectively.

2.2. Chemical and morphological characterization of TPs

TPs' main bulk chemical features were obtained by μ-FTIR using Thermo Scientific Nicolet iN10 equipment (Madison, WI, USA). The spectra were collected using a Ge tip ATR, and acquisition was carried out with an MCT-A detector using 64 scans from 4000 to 675 cm^{-1}. Spectral data were examined using the OMNIC Picta software (Waltham, MA, USA). The morphological analysis of TP was conducted by Scanning Electron Microscopy (HITACHI TM 3000 Tabletop, Tokyo, Japan), according to the previously described method (Savino et al., 2022).

2.3. Metal analysis of TPL

TPL was screened for a quantitative determination of metal content by Inductively Coupled Plasma Mass Spectrometry (ICP-MS iCAP Q Thermo Fisher spectrometer) according to the EPA Method (EPA, 1998). The leachate (three replicates) and blank sample (FNSW) were acidified with nitric acid (HNO_3) and then frozen at −20 °C. Samples were diluted with milli-Q distilled water to obtain a proper concentration for ICP-MS analysis. A mix of internal standards contained 45Sc, 73Ge, 103Rh, 115In, and 159 Tb in nitric acid 10 % was used. The samples were analysed using the isotopes ^{9}Be, ^{27}Al, ^{48}Ti, ^{51}V, ^{52}Cr, ^{55}Mn, ^{56}Fe, ^{59}Co, ^{60}Ni, ^{63}Cu, ^{66}Zn, ^{75}As, ^{78}Se, ^{111}Cd, ^{118}Sn, ^{121}Sb, ^{205}Tl, Medium Pb (206,207 and 208). The concentration value was expressed as an average (N = 3) μg/L ± SD (Standard Deviation). These metals were chosen based on their use in the production of synthetic polymers and their known toxic effects.

2.4. Untargeted screening of organic compounds in TPL

The screening of the organic compounds of TPL was carried out by LC-HRMS. Compounds released from TPs were first extracted with methanol, 50 mg/0.5 ml for five minutes, and the extract was analysed to annotate the main compounds. The molecules released into seawater were first concentrated by solid-phase extraction (SPE). Three replicates of TPL and blank sample (FNSW) were analysed using Waters Oasis® PRiME HLB 3 cc cartridges, 150 mg, Milford, U.S.A (for details see Supplementary Material, section S1). All extracts were analysed using an UltiMate 3000 UHPLC system coupled to an Orbitrap Elite mass spectrometer (Thermo Scientific, Bremen, Germany) equipped with a heated electrospray ion source (HESI-II) or an Atmospheric pressure chemical ionization source (APCI) (Thermo Scientific, Bremen, Germany).

Analyses were performed following a protocol similar to that used to determine additives and degradation products of microplastics (Costa et al., 2024). The chromatographic separation was achieved using a Thermo Scientific Accucore RP-18 (2.1 × 100 mm, 2.6 μm) column with a mobile phase composed of water (A)/methanol (B) for APCI and water (A)/acetonitrile (C) for ESI, all solvents with 0.1 % formic acid. The gradient (in v/v %) started with 20 % of B for 1 min. Then B increased linearly to 60 % in 8 min and then to 100 % of B in 14 min. This composition was maintained for 6 min, and then the mobile phase was returned to 20 % B in 1 min, and this composition was maintained for an additional 4 min before the next run. The same program was used under ESI, but the organic solvent was acetonitrile with 0.1 % formic acid (C). The flow rate was 0.3 mL/min. The sample injection volume was 10 μL. The acquisition was performed in data-dependent mode using Collision Induced Dissociation (CID) or High-energy Collision Dissociation (HCD) activation with dynamic exclusion under positive and negative polarity. The main ionization and ion optics parameters under APCI were the following: vaporizer temperature 380 °C; sheath gas flow 30 arbitrary

units; auxiliary gas flow 20 arbitrary units; capillary temperature 350 °C; source current 5 mA; S-Lenses RF level, 69 %. The scan range was 100–1000 *m/z*. Under HESI, the parameters were the following: heater temperature 350 °C; sheath gas flow 35 arbitrary units; auxiliary gas flow 5 arbitrary units; capillary temperature 350 °C; spray voltage 3.2 kV; S-Lenses RF level, 69 %. Scan range was 100–1000 *m/z*.

LC–MS data analysis was performed using Xcalibur 4.1 (Thermo Scientific, Bremen, Germany). Annotation of compounds was carried out using Compound Discoverer 3.3 (Thermo Scientific, Bremen, Germany), which possesses a comprehensive, integrated set of libraries and databases allowing for compound annotation and detection of statistical differences between samples. Profiles were processed using identification workflows, including access to local and online databases such as mzCloud, extractables, and leachables HRAM. Compounds showing an mzCloud match above 85 % were reported.

2.5. Animal and gamete collection

Adult Mediterranean mussels *Mytilus galloprovincialis* of 5–6 cm in length were collected from an aquaculture plant located in the Mar Grande of Taranto (Ionian Sea) and transported in a cool box to the Marine Biological Resources service of Stazione Zoologica where animals were acclimated for one week in tanks filled with running natural seawater (NSW, salinity 40 g/l, pH 8.2 ± 0.1, temperature 18 °C) and equipped with oxygen pumps. After the acclimation period, the mussels were induced to spawn using a thermal shock procedure by moving them alternately in seawater baths at 15 ± 1 °C and 20 ± 2°C for 30 min each. Spawning mussels were isolated individually in 250 ml beakers filled with FNSW and left to spawn for 15 min. After spawning, oocyte and sperm solutions were filtered with 50 μm and 80 μm sieves to remove debris, and then gamete quality was preliminarily checked by microscopic visualization to evaluate the morphology of the oocytes and motility and concentration of spermatozoa. For each individual, gametes were divided into two glass tubes for exposure: FNSW (control, CTRL) and TPL. Exposure was maintained for 1 h and 2 h at 18 °C with shaking, and immediately after exposure, gametes were used for physiological analyses.

2.6. Gamete quality assessment

After exposure, physiological parameters of gamete quality were assessed using fluorescent staining coupled with fluorescence spectroscopy. For each parameter, a specific fluorochrome was employed, and the fluorescence spectra were recorded using a spectrofluorometer (Shimadzu RF-5301, Tokyo, Japan) for spermatozoa and a microplate reader (Tecan Infinite® m1000 pro) for the oocytes. Moreover, for spermatozoa, motility was also evaluated.

2.6.1. Sperm motility

Sperm motility was assessed using the Computer-assisted sperm analysis system Sperm Class Analyzer (SCA® CASA, MICROPTIC S.L., Barcelona, Spain, software version 4.0) coupled to a phase contrast microscope (Nikon Eclipse model 50i; negative contrast). After exposure, spermatozoa were diluted in FNSW, and 10 μl of this solution was placed on a drop-loaded slide (Sefi Medical Instruments, Haifa, Israel) and evaluated under the microscope. A minimum of 3 fields and 200 sperm tracks were analysed.

2.6.2. Viability

Viability of the male and female mussel gametes was evaluated, respectively, by employing the LIVE/DEAD Sperm Viability Kit (Life Technologies, Milan, Italy), which consists of two dyes, SYBR-14 and propidium iodide (PI), and the fluorochrome SYBR green in combination with PI. The SYBER-14 and the SYBER green penetrate gametes with intact membranes, emitting a bright green fluorescence. On the other hand, PI only penetrates the cells that have lost membrane integrity and emits in the red fluorescence range. Aliquots of oocytes (1000 oocytes/mL) and spermatozoa (5×10^6 cells/mL) were stained by adding 100 mM of SYBR green and SYBER-14, respectively, and were incubated for 15 min in the dark at 18 ± 1 °C. Thereafter, 12 μM PI was added, and samples were further incubated for 15 min at 18 ± 1 °C in the dark. Finally, SYBR 14 and PI fluorescences intensity were measured, respectively, by setting the excitation wavelengths at 488 nm and 545 nm and recording the emission spectra in the range of 500–560 nm and 570–700 nm, by using the microplate reader for the oocytes and spectrofluorimetry for spermatozoa (Gallo et al., 2018a; Gallo et al., 2022).

2.6.3. Mitochondrial activity

The mitochondrial dye 5′,6,6′-tetrachloro-1,1′,3,3′-tetraethylbenzimidazolylcarbocyanine iodide (JC-1; ThermoFisher Scientific, Milan, Italy) was used to evaluate the mitochondrial membrane potential (MMP). JC-1 is a lipophilic dye that enters selectively into mitochondria and remains in a monomeric form, emitting in the green wavelength range (525–530 nm) if the MMP is low. Under high MMP values, JC-1 forms J-aggregates, which lead to orange/red emission (~595 nm) (Reers et al., 1995). The red and green fluorescence ratio is considered a direct assessment of mitochondrial activity.

For the fluorescence staining of spermatozoa, aliquots of 1×10^6 spermatozoa/mL were incubated for 30 min with 5 μM JC-1 in the dark at 18 °C. Samples were then centrifuged at 900 *g* at 4 °C for 10 min, the pellet was re-suspended in FNSW and incubated for an additional 30 min under the same conditions. Finally, the pellets were resuspended in 900 μL of FNSW and analysed in duplicates using the spectrofluorometer. For the oocytes, the fluorescence staining procedure was similar except for the centrifugation step. Oocyte pellets were suspended in 600 μL FNSW and split into three wells of the 96 multi-well plate to read them in triplicate. A stained aliquot of control spermatozoa or oocytes was incubated in 5 μM CCCP (Carbonyl cyanide 3-chlorophenylhydrazone; Merck Life Science) to prepare a positive control. Fluorescence emission spectra were recorded at emission wavelengths from 500 to 620 nm by exciting at 488 nm. The MMP was calculated as a ratio of the fluorescence peak values at ~595 nm and ~525 nm.

2.6.4. Oxidative status

Intracellular ROS were detected employing the fluorochrome 2′,7-dichlorodihydrofluorescein diacetate (H_2DCF-DA). For the fluorescence staining of spermatozoa, aliquots of 5×10^6 spermatozoa/mL were incubated in 10 μM H_2DCF-DA at 18 °C for 30 min in the dark. After staining, the cells were pelleted by centrifugation at 900 *g* and then suspended in FNSW for an additional 30 min under the same conditions. Finally, spermatozoa were washed, re-suspended in 900 μL of FNSW, and analysed in duplicate. An aliquot of control spermatozoa was incubated with hydrogen peroxide (25 μM) for 1 h before staining and used as a positive control. Oocyte staining was performed applying the same procedure, excluding centrifugations. Oocyte pellets were suspended in 600 μL FNSW and split into three wells of the 96 multi-well plate to read them in triplicate.

Emission spectra were recorded between 500 and 560 nm by setting the excitation wavelength at 488 nm.

Lipid peroxidation was assessed using the fluorescent membrane probe C11-BODIPY581/591, an oxidation-sensitive fluorophore that functions as a fatty acid analogue. This probe is easily incorporated into membranes and exhibits a shift in fluorescence from red (590 nm) to green (510 nm) upon oxidation. Sperm suspensions were incubated in the dark at 18 °C for 30 min with 5 μM C11-BODIPY$^{581/591}$ dissolved in DMSO. After staining, the spermatozoa were centrifuged at 900 *g* for 15 min, resuspended in FNSW, and transferred to a quartz cuvette for spectrofluorimetric analysis.

Oocyte staining was carried out using the same procedure, except for the centrifugation steps. The oocyte pellets were resuspended in 600 μL of FNSW and distributed into three wells of a 96-well plate for triplicate readings.

Positive controls were prepared by incubating the gamete samples with two peroxidation promoters (150 mM ferrous sulfate and 750 mM vitamin C). Fluorescence intensity was measured with 488 nm excitation and emission wavelengths between 500 and 650 nm. A ratiometric analysis was then performed by comparing the fluorescence emission peak at approximately 520 nm to the sum of the emission peak values at ~520 nm and ~590 nm.

2.6.5. Intracellular pH

The pH_i was measured using the pH-sensitive fluorescent dye 2′,7′-bis-(2-carboxyethyl)-5-(and-6) carboxyfluorescein acetoxymethyl ester (BCECF-AM) from Life Technology in Milan, Italy. This dye can cross the cell membrane and is converted by esterases inside the cell into BCECF, which emits fluorescence depending on the pH level. Oocytes were loaded with the ester form of BCECF (5 μM BCECF-AM) and incubated in the dark at 18 °C for 30 min. After washing, the oocytes were suspended in FNSW and placed in a 96-well plate for spectrofluorometric analysis. The pH was determined by exciting the samples alternately at 440 nm and 490 nm and calculating the ratio of the fluorescence emission peak values at 535 nm. This ratio was converted into pH values using a calibration curve constructed for each experiment by incubating oocyte samples in a calibration buffer solution with different pH levels (6.5, 7.2, and 8.0) in the presence of 5 μM nigericin (Sigma Aldrich, Milan, Italy). The latter promotes the K^+/H^+ exchange equilibrating intracellular and extracellular pH, resulting in a linear relationship between fluorescence intensity and pH. The calibration equation allowed the conversion of emission peak ratios obtained from excitation at 440 nm and 490 nm into pH values.

2.7. Statistical analysis

Each gamete's physiological parameter was analysed in five samples of male and female gametes, and all measurements were performed in triplicate. Each data set was tested for normality and homogeneity of variance by the Shapiro-Wilks test and Levene's test, respectively. Statistical comparisons were conducted using the software Systat 11.0 (Systat Software Inc.) to perform the one-way variance analysis (ANOVA) followed by Fisher's Least Significant Differences (LSD) test as a multiple comparison post hoc test. The minimum level of significance was set at $p < 0.05$. The data are reported as mean ± SD.

3. Results

3.1. Chemical and morphological characterisation of TPs

The chemical characterisation of the TPs by FTIR-ATR technology highlighted some characteristic bands of the SBR copolymer (Fig. 1). The absorption bands between 3100 cm^{-1} and 2800 cm^{-1} were assigned to C—H stretching, in agreement with a structure possessing alkyl and aromatic C—H bonds. Signals between 1670 cm^{-1} and 1540 cm^{-1} are characteristic of the C═C bonds of SBR but have also been detected for natural rubber. Signals between 1500 cm^{-1} and 1300 cm^{-1} are related to the C—H bending typical of rubber. The absorbance between 1370 and 1070 cm^{-1} was assigned to chemical groups possessing S—O, S═O and S—C bonds. The broad absorbance observed for TPs in this region indicates the presence of sulfur and, therefore, of bonds associated with the vulcanization process. The signals between 1000 and 800 cm^{-1} are related to C═C bonds from butadiene in the SBR. The broad absorbance above 3100 cm^{-1} was assigned to O—H vibrations.

The ultrastructural analysis of the surface morphology of TPs fragments showed an irregular and jagged shape of particles, which might be due to the pulverization/grinding process of used tires (Fig. 2).

3.2. TPL metals analysis

The ICP-MS analysis revealed the presence of several inorganic elements in TPL (see Table 1). In particular, high concentrations of Zn and Ti were observed, while metals such as Mn, Tl, Co and Pb were detected at lower concentrations (<50 μg/L) in TPL and in trace amounts in the seawater control. Other metals, such as Be, Al, V, Cr, Fe, Ni, Cu, As, Se,

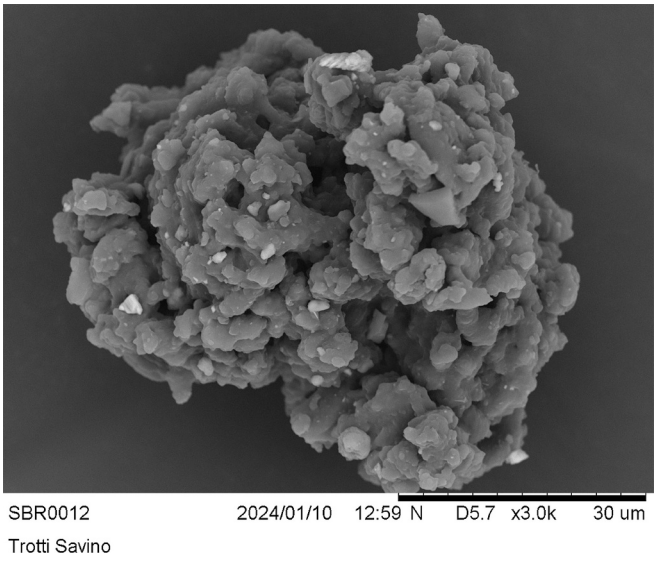

Fig. 2. Scanning Electron Microscopy Analysis of tire rubber particles.

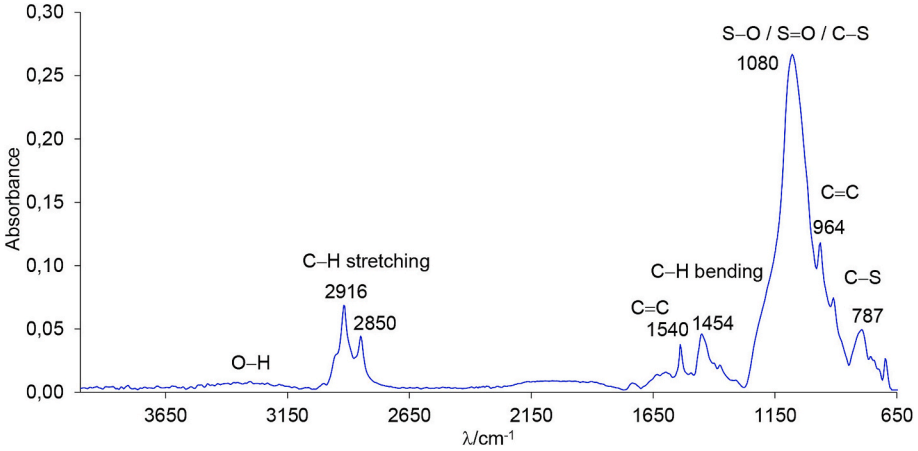

Fig. 1. The IR spectrum of Styrene Butadiene Rubber (SBR) copolymer acquired by FTIR-ATR.

Table 1
Metal concentrations (μg/L) measured in tire particle seawater leachate (TPL) and in filtered natural seawater (CTRL) by ICP-MS. LOQ: Limit of Quantification value (μg/L). The Standard Deviation (±SD) was calculated for triplicate TPL samples.

Metal	LOQ	CTRL	TPL
μg/L			
Be	0.34	<LOQ	<LOQ
Al	1.75	<LOQ	<LOQ
Ti	0.43	<LOQ	767.42 ± 2.13
V	0.22	<LOQ	<LOQ
Cr	1.73	<LOQ	<LOQ
Mn	0.54	1.29	49.91 ± 1.99
Fe	7.24	<LOQ	<LOQ
Co	0.24	<LOQ	24.50 ± 0.31
Ni	0.53	<LOQ	<LOQ
Cu	2.70	<LOQ	<LOQ
Zn	0.95	1.46	3266.07 ± 158.62
As	0.09	<LOQ	<LOQ
Se	1.13	<LOQ	<LOQ
Cd	0.41	<LOQ	<LOQ
Sn	0.11	<LOQ	<LOQ
Sb	0.10	<LOQ	<LOQ
Tl	1.10	1.21	24.11 ± 0.01
Pb	0.99	0.59	19.09 ± 2.96

Cd, Sb and Sn showed concentrations below the Limit of Quantification value (LOQ).

3.3. Untargeted screening of organic compounds in TPL

The untargeted analysis of the organic molecules leaching from the tire particles disclosed the presence of several compounds containing nitrogen in their structure (Table 2). These included benzothiazoles (BTH, 2-ABTH, 2-OH-BTH), quinolones, amines (Diphenylamine, DCHA, IPPD, CPPD, 6PPD, DTPD), and amides (MA, EC, PEA, oleamide, stearamide, DCBS), among others. The detected compounds can be grouped into three categories: compounds resulting from the vulcanization process, antioxidants and protective agents. A typical full scan profile of a methanolic extract obtained under positive polarity showed the presence of a main compound at 11.80 min with *m/z* 269.201 (Supplementary materials, section S2). This exact mass as well as the CID fragmentation (Table 2) fits to 6PPD (N-(1,3-Dimethylbutyl)-N'-phenyl-p-phenylenediamine. 6PPD was not detected in seawater extracts, while its quinone product was observed in trace amounts (Supplementary materials, section S3). Some compounds detected in the methanolic extracts were not observed in seawater (Table 2).

3.4. Sperm quality assessment

Exposure of male gametes to TPL altered their motility and mitochondrial activity (Fig. 3). After TPL exposure, the sperm motility significantly decreased from 84.7 ± 1.2 to 22.4 ± 1.0 after 1 h and from 72.7 ± 0.9 to 11.6 ± 0.2 after 2 h. On the other hand, in spermatozoa exposed to TPL, MMP values significantly raised from 11.3 ± 1.2 to 16.2 ± 2.2 after 1 h and from 11.3 ± 2.2 to 22.3 ± 2.3 after 2 h exposure (Fig. 3). Moreover, MMP significantly increased with increasing exposure time (Fig. 3).

Conversely, sperm viability and oxidative status were not impaired by TWPL exposure. Both intracellular ROS levels and plasma membrane lipid peroxidation did not significantly change after sperm exposure to TPL for 1 h and 2 h (Table 3). Similarly, the pH_i was not significantly affected (Table 3).

3.5. Oocyte quality assessment

The mitochondrial activity was also affected in female gametes. While unexposed oocytes show MMP values of 1.80 ± 0.3 and 1.61 ± 0.1 after 1 and 2 h in FNSW, TPL exposure for the same time induced an increase of the values to 4.13 ± 0.4 and 5.45 ± 0.5, respectively (Fig. 4). Furthermore, MMP showed a significant increase with the exposure time (Fig. 4). As observed for male gametes, the intracellular ROS level, plasma membrane lipid peroxidation and the pH_i were not significantly influenced by TPL exposure (Table 4).

4. Discussion

The present study assessed the organic compounds and metal profiles of seawater leachates produced from end-of-life car tires and the associated adverse effects on the gamete quality of the Mediterranean mussel *Mytilus galloprovincialis*. Tire particles were exposed to FNSW for ten days under controlled conditions. The release of chemical compounds from the tire particles is expected to occur gradually over this exposure period, with some compounds likely leaching more quickly than others. The release rates may vary depending on the specific additives, their chemical properties, and physical factors such as temperature and salinity. In this study, the TPL was collected after ten days of stirring at 18 °C, which provides insight into the potential long-term leaching behaviours of these compounds in seawater. Metal analysis reveals the presence of the following elements in TPL: Zn, Ti, Mn, Tl, Co, and Pb. Tires commonly contain 13 % to 16 % metals, used in tire manufacturing as stabilizers and additives (Senin et al., 2016). Among the metals detected in TPL, Zn showed the largest content. This result is consistent with the high Zn content in tires, which is known to be about 1–2 % of the total weight (Degaffe and Turner, 2011). Some studies have also reported high contents of Zn leaching from tire rubber (Capolupo et al., 2020; Halsband et al., 2020). Indeed, Zn is employed in the vehicle tire manufacturing industry mainly as ZnO and ZnS, which are activators and accelerators of the vulcanization process, promoting the formation of rubber cross-linking (Degaffe and Turner, 2011). The presence of other metals, such as Pb and Tl, is also associated with their use as accelerators of the vulcanization process (O'Loughlin et al., 2023). In contrast, Co, Mn and Ti are commonly involved in the catalysis for the polymerization of butadiene rubber (Rackaitis and Graves, 2017). Through leaching, tire particles have been noted to modify seawater chemistry. It has been demonstrated that tire wear particles can release heavy metals that may contribute to pH changes in marine environment (Capolupo et al., 2020; Halsband et al., 2020).

Untargeted analysis of TPL allowed the annotation of a broad range of organic additives, mainly antioxidants, and vulcanizing and protective agents. In particular, most of the annotated organic compounds, such as BTH and its derivates (2-A-BTH, 2-OH-BTH), MA, EC, DCHA, DFG, DCU, and DCBS, are commonly employed as vulcanization accelerators in rubber production (Jeong et al., 2022; Stack et al., 2023; Zhang et al., 2023). BTH and its derivatives also act as corrosion inhibitors and UV stabilizers (Johannessen et al., 2022). The non-target screening also revealed the presence of 6PPD-quinone in the TPL. This compound is a by-product of a common tire manufacturing additive used as an antioxidant and antiozonant, which prevents the rubber from cracking due to exposure to oxygen, ozone, and temperature changes (Hua and Wang, 2023). Moreover, δ-Valerolactam, a monomer of Nylon 5, was also detected. This is likely due to the employment of Nylon 5 as a reinforcement of the tire strings to provide good adhesion and shock absorption. Additionally, other derivatives of BTH and various other additives have been found in seawater leachates from TPL, as reported in previous studies (Capolupo et al., 2020; Yang et al., 2022). It should be noted that some compounds observed in the studied methanolic extracts were not detected in seawater, which could be related to their low solubility or chemical degradation.

It is important to note that the level of metal and organic compounds detected in seawater leachate may also be influenced by additional contributors from the on-road collection environment. Indeed, as tires roll on roads, through various mechanisms they can adsorb different contaminants, including heavy metals (Pb, Tl, Zn) from road dust and

Table 2
Annotated organic compounds from tire particle leachates (TPL). Annotation was achieved using TP methanolic extracts. The compounds annotated in the methanol extracts were searched in TPL extracts. The tire additive class was reported for each compound. * Annotation based on the mzCloud, Massbank databases and/or mass spectral data (*m/z* values, isotope distributions and fragmentation patterns (CID or HCD). Mobile phase composed of water and methanol (APCI source). "X" Compound not found in TPL; "√" Compound found in TPL.

Compound name	Formula	*m/z* (polarity)	Annotation/Identification*	TPL	Tire additive class
δ-Valerolactam	C_5H_9NO	100.075 (+)	m/zCloud 98.7 %	X	Reinforced rubber
Melamine (MA)	$C_3H_6N_6$	127.073 (+)	m/zCloud 98.8 %	√	Vulcaniser in tire production
Isoquinoline	C_9H_7N	130.065 (+)	m/zCloud 99.2 %	X	Antioxidant
Benzothiazole (BTH)	C_7H_5NS	136.022 (+)	m/zCloud 97.0 %	√	Vulcanization accelerator, ultraviolet light absorber
N-Cyclohexylacetamide (EC)	$C_8H_{15}NO$	142.122 (+)	HCD − 114 (16) 98 (20) 60 (100)	√	Vulcanization accelerator
6-Methylquinoline	$C_{10}H_9N$	144.081 (+)	m/zCloud 91.5 %	√	Antioxidants
2-Aminobenzothiazole (2-ABTH)	$C_7H_6N_2S$	151.032 (+)	m/zCloud 93.6 %	√	Vulcanization accelerator
2-Hydroxybenzothiazole (2-OH-BTH)	C_7H_5NOS	152.017 (+)	m/zCloud 96.8 %	√	Vulcanization accelerator
2,6-Dimethylquinoline	$C_{11}H_{11}N$	158.096 (+)	HCD − 143 (100) 115 (78) 91 (31) Massbank	X	Antioxidants
Diphenylamine	$C_{12}H_{11}N$	170.096 (+)	m/zCloud 96.3 %	√	Antioxidant
2,2,4-Trimethyl-1,2-dihydroquinoline	$C_{12}H_{15}N$	174.127 (+)	HCD − 158 (49) 144 (100) 130 (46) 117 (46) 115 (17) 91 (34) Massbank	√	Protective additive (antiozonant/ antioxidant/heat protectant) Mass bank
Acridine	$C_{13}H_9N$	180.080 (+)	m/zCloud 99.2 %	X	Antioxidant
Dicyclohexylamine (DCHA)	$C_{12}H_{23}N$	182.190 (+)	HCD − 100 (100) 83 (76) 55 (2) Massbank	√	Vulcanization accelerator Mass Bank
2-Phenoxyaniline	$C_{12}H_{11}NO$	186.091 (+)	CID − 168 (100) 108 (26) 93 (30)	√	–
Iminostilbene	$C_{14}H_{11}N$	194.096 (+)	m/zCloud 94.5 %	X	Antioxidant
2-Phenylbenzimidazole	$C_{13}H_{10}N_2$	195.091	m/zCloud 89.9 %	√	Ultraviolet light absorber
N-Octyl-2-pyrrolidone	$C_{12}H_{23}NO$	198.185 (+)	m/zCloud 95.5 %	√	–
Unknown	$C_{14}H_{14}N_2$	211.122 (+)	CID − 194 (88) 184 (100) 169 (80) 118 (61)	X	–
Unknown	$C_{13}H_9NS$	212.052 (+)	HCD − 109 (100) 104 (3)	X	–
N,N'-Diphenylguanidine (DFG)	$C_{13}H_{13}N_3$	212.118 (+)	m/zCloud 95.1 %	√	Vulcanizing agent
N,N'-Dicyclohexylurea (DCU)	$C_{13}H_{24}N_2O$	225.195 (+)	m/zCloud 99.7 %	√	Vulcanization accelerator
Drometrizole	$C_{13}H_{11}N_3O$	226.097 (+)	m/zCloud 97.0 %	√	Ultraviolet light absorber and antioxidant
N-Isopropyl-N'-phenyl-p-phenylenediamine (IPPD)	$C_{15}H_{18}N_2$	227.154 (+)	m/zCloud 95.7 %	X	Rubber antiozonant
Hexadecanamide (PEA)	$C_{16}H_{33}NO$	256.263 (+)	m/zCloud 97.5 %	X	Bio-modifier and surface activator rubber
N-cyclohexyl-N'-phenyl-p-phenylenediamine (CPPD)	$C_{18}H_{22}N_2$	267.185 (+)	CID – 224 (11) 211 (16) 183 (100) 166 (17)	X	Protective additive (antiozonant/ antioxidant/heat protectant
N-(1,3-Dimethylbutyl)-N'-phenyl-p-phenylenediamine (6PPD)	$C_{18}H_{24}N_2$	269.201 (+)	CID − 192 (32) 185 (100) 184 (78)	X	Protective additive (anti-aging agent/ antiozonan)
Oleamide	$C_{18}H_{35}NO$	282.278 (+)	m/zCloud 98.2 %	√	Improve compounding process and abrasion resistance
Stearamide	$C_{18}H_{37}NO$	284.294 (+)	m/zCloud 94.4 %	√	Improves the physical properties of rubber
Unknown	$C_{20}H_{18}N_2$	287.155 (+)	CID − 195 (6) 181 (59) 180 (100)	√	–
N,N'-Bis(2-methylphenyl)-1,4-benzenediamine (DTPD)	$C_{20}H_{20}N_2$	9.169 (+)	HCD − 197 (60) 182 (29) 181 (65) 180 (100) 107 (25) 106 (40)	X	Protective additives
2-((4-Methylpentan-2-yl) amino)-5-(phenylamino) cyclohexa-2,5-diene-1,4-dione (6PPD-quinone)	$C_{18}H_{22}N_2O_2$	299.175 (+)	CID − 256 (100) 243 (44) 241 (30) 215 (81) 200 (32) 187 (17)	√	Degradation product of 6PPD
Unknown	$C_{23}H_{26}N_2$	331.217 (+)	HCD − 258 (35) 184 (18) 171 (45) 158 (100)	X	–
N,N-Dicyclohexyl-2-benzothiazolsulfene amide (DCBS)	$C_{19}H_{26}N_2S_2$	347.161 (+)	CID − 265 (64) 180 (100)	X	Vulcanizing additive (vulcanization accelerator)

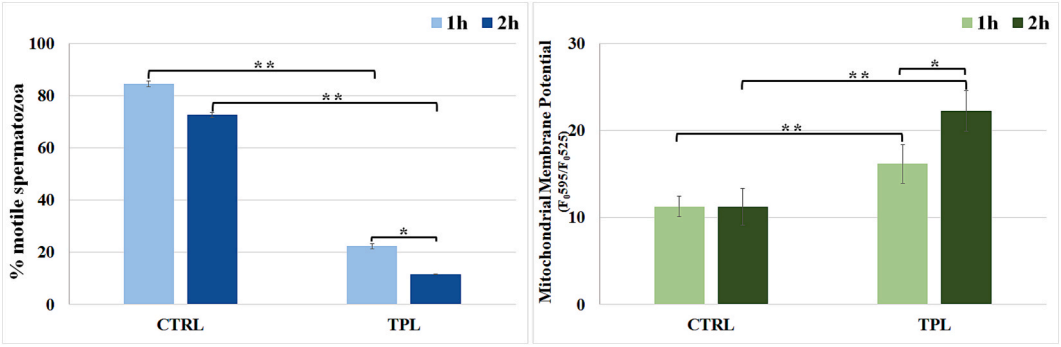

Fig. 3. Sperm motility percentage and mitochondrial membrane potential values recorded in *Mytilus galloprovincialis* spermatozoa exposed for 1 and 2 h to filtered natural seawater (CTRL) and tire particle leachate (TPL). * and ** indicate significant and high significant differences, respectively.

Table 3
Values of viability, intracellular reactive oxygen species (ROS), plasma membrane lipid peroxidation (LPO) and intracellular pH (pH_i) recorded for *Mytilus galloprovincialis* spermatozoa exposed to filtered natural seawater (CTRL) and tire particle leachate (TPL) for 1 and 2 h.

	CTRL		TPL	
	1 h	2 h	1 h	2 h
Viability	81.1 ± 0.5	80.4 ± 0.7	79.6 ± 1.5	78.7 ± 2.2
ROS	28.5 ± 3.2	25.8 ± 3.2	26.6 ± 2.1	28.9 ± 1.7
LPO	27.3 ± 1.7	28.3 ± 1.2	27.7 ± 2.6	27.9 ± 2.1
pH_i	9.4 ± 0.4	9.6 ± 0.3	9.4 ± 0.4	9.7 ± 0.2

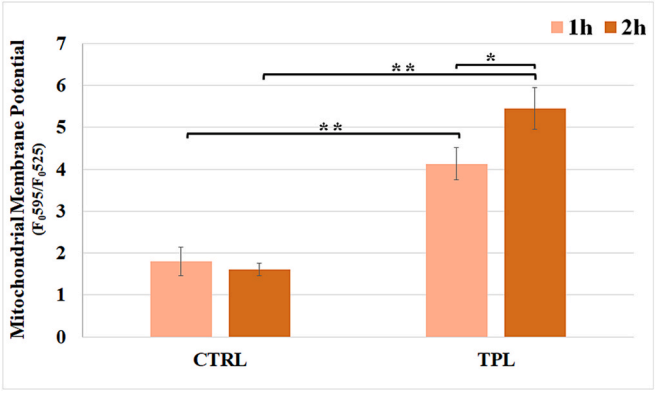

Fig. 4. Mitochondrial Membrane Potential values recorded in *Mytilus galloprovincialis* oocytes exposed for 1 and 2 h to filtered natural seawater (CTRL) and tire particle leachate (TPL). * and ** indicate significant and high significant differences, respectively.

Table 4
Values of viability, intracellular reactive oxygen species (ROS), plasma membrane lipid peroxidation (LPO) and intracellular pH (pH_i) measured for *Mytilus galloprovincialis* oocytes exposed for 1 and 2 h to filtered natural seawater (CTRL) and tire particle leachate (TPL).

	CTRL		TPL	
	1h	2h	1h	2h
Viability	81.7 ± 2.9	77.8 ± 2.5	78.7 ± 3.5	77.0 ± 2.6
ROS	124.9 ± 26.9	132.5 ± 24.2	116.5 ± 13.9	123.0 ± 18.5
LPO	25.9 ± 6.5	20.4 ± 4.4	24.7 ± 5.1	19.6 ± 1.7
pH_i	7.8 ± 0.08	7.7 ± 0.1	7.9 ± 0.1	7.8 ± 0.03

brake wear, and organic compounds from road surfaces and atmospheric deposition. The contaminant adsorption is affected by several factors as tire composition, road surface conditions, traffic volume and speed, and environmental conditions. As a result, leachate composition can be highly variable.

The organic chemical and metal profiles reveal that the seawater TPL is a complex mixture of different chemical compounds, some of them of established toxicity, which may be released into the marine environment through leaching, contributing to seawater contamination. The toxicity of freshwater leachate produced from end-of-life car tires was intensively investigated using several species, leading to the uncovering of various effects, which have been attributed to differences in tire composition, leachate generation method and species sensitivity (Wagner et al., 2018; Wik and Dave, 2009). Conversely, the potential toxicity of end-of-life car tire seawater leachate to marine organisms is far less studied (Halsband et al., 2020). Examples include the exposure to end-of-life car tire leachate has been demonstrated to reduce the efficiency of photochemical energy conversion of macroalgae (Turner and Rice, 2010), growth inhibition in microalgae (Capolupo et al., 2020), behavior alteration in shrimps (Siddiqui et al., 2022), and high mortalities in marine copepods (Halsband et al., 2020; Yang et al., 2022). There is also very limited toxicity information on marine invertebrate reproduction. Tire wear particle leachate has been proven to affect the growth, reproduction and sex ratio of copepods (Yang et al., 2025) and shorten the reproductive period of rotifers, slow down their swimming speed, and reduce the number of offspring (Lian et al., 2025).

In the Pacific oyster *Crassostrea gigas*, the viability and ROS production of spermatozoa and oocytes, as well as the fertilization and embryo development, were demonstrated to be not affected by exposure to the leachates issued from end-of-life car tires (Tallec et al., 2022b). In the Mediterranean mussel *M. galloprovincialis*, leachates produced from car tire rubber reduced fertilization success after sperm pre-exposure and impaired embryo development (Capolupo et al., 2020). In the present study, we investigated the sensitivity of mussels' early life stages, such as spermatozoa and oocytes, to the chemical compounds leached into seawater from end-of-life car tire particles by evaluating in both gametes different markers closely linked with the reproductive function, such as viability, mitochondrial activity, intracellular reactive oxygen species levels, plasma membrane lipid peroxidation, and pH_i. Moreover, sperm motility was also checked. The obtained data indicate that end-of-life car tire seawater leachate significantly decreases sperm motility and increases mitochondrial activity in male and female gametes. On the other hand, as previously observed for oyster gametes, TPL did not affect intracellular ROS levels and lipid peroxidation (Tallec et al., 2022b), despite the high levels of Zn detected. Concerning this aspect, it is hypothesized that these levels did not significantly affect these parameters because the detected levels did not exceed the toxicity threshold for Zn, likely due to compensatory mechanisms such as increased zinc binding, sequestration in cells, or upregulation of transport proteins, which ensure that the zn-buffering capacity of gametes is not exceeded.

Mitochondrial functionality is one of the main indicators used for estimating gamete quality. In *M. galloprovincialis* spermatozoa,

mitochondria are located below the sperm head (Boni et al., 2016), and proper mitochondrial functionality has been widely demonstrated to be required for ensuring high sperm quality (Amaral et al., 2013). Indeed, structural and functional mitochondrial alterations following sperm exposure to several physical and chemical stressors have been related to the loss of sperm function, confirming the crucial role played by these organelles in sperm quality (Gallo et al., 2016; Gallo et al., 2018b; Gallo et al., 2018c). On the other hand, in the oocyte, the number, distribution, and activity of mitochondria are narrowly tied to oocyte quality, playing a central role in the cellular metabolism providing energy for successful cytoplasm and nucleus maturation, fertilization, and embryo development (Bezzaouia et al., 2014; Gallo et al., 2022). Thereby, any stressor affecting mitochondrial functionality might impair oocyte competence.

In this study, we demonstrated for the first time that the mitochondrial activity of mussel gametes, assessed as MMP, increased after exposure to TPL. This result suggests that exposure to leachate alters the energy demand, leading to an increase in MMP, which has been demonstrated to be positively correlated with ATP production. Moreover, it has been shown that the mitochondria-derived ATP is crucial for activating many enzymes and chemical reactions involved in stress response (Picard et al., 2018).

ATP is also the main energy source used by the flagellum to initiate and propagate the motility of spermatozoa. Although the present study suggests an increase in ATP production following sperm exposure to end-of-life car tire leachate, a decrease in motility was conversely observed. This is because in *M. galloprovincialis* spermatozoa, the mitochondria-derived ATP is not involved in sperm motility, probably because glycolysis is the main energy source for sperm motility in this marine species (Gallo et al., 2021).

Motility is considered a reliable predictor of sperm quality since it is an essential prerequisite to ensure the fertilization process. In a previous study, the pre-exposure of *M. galloprovincialis* spermatozoa to end-of-life car tire seawater leachate has been proven to decrease fertilization success. The authors proposed that the observed fertilization success decrease can be due to alterations in cellular structures that regulate the energetic metabolism and motility of spermatozoa (Capolupo et al., 2020). The present study supports this suggestion and sheds light on the importance of gamete quality assessment in investigating the toxicity of environmental contaminants to gain new insights into their mechanisms of action.

5. Conclusion

The present study provides novel insights into the reproductive toxicity of tire particle leachates (TPL) in *Mytilus galloprovincialis*. Exposure to TPL led to a significant increase in mitochondrial activity, by approximately 25 % in oocytes and 30 % in spermatozoa, alongside a substantial reduction in sperm motility of around 40 %. These physiological impairments suggest a serious risk to reproductive success in this species. Chemical analysis of leachates identified several contaminants, with zinc being the most prevalent metal (~3 mg/L), along with a suite of organic additives, including antioxidants and vulcanizing agents, all of which are likely contributors to the observed toxic effects. The complexity of the leachate mixture, coupled with the formation of toxic degradation products and the potential for a "cocktail effect," complicates the identification of specific toxicants responsible for the reproductive toxicity. This underscores the need for more targeted research to characterize individual and combined chemical impacts. Moreover, the limitation of the current study to a single species, *M. galloprovincialis*, and the use of laboratory-based exposure, which may not fully capture the complexities of real-world environmental conditions, highlights the need for future studies on the effects of TPL including multiple species and environmentally relevant exposure scenarios to better understand the ecological risks.

In conclusion, the growing accumulation of waste tires in marine environments presents new threats to marine organisms, compromising their reproductive health and ultimately endangering the survival of marine species and, consequently, marine biodiversity. To mitigate these risks, concerted efforts are needed to ensure environmental safety. Strategies such as improving waste management practices, reducing tire leachate release, and enhancing water quality monitoring could help minimize adverse effects on marine biota.

CRediT authorship contribution statement

Ilaria Savino: Writing – review & editing, Writing – original draft, Methodology, Investigation, Formal analysis, Conceptualization. **Amir Nobahar:** Writing – review & editing, Investigation, Formal analysis. **José P. Da Silva:** Writing – review & editing, Methodology, Funding acquisition, Data curation, Conceptualization. **Pietro Cotugno:** Writing – review & editing, Supervision, Methodology, Investigation, Data curation. **Rosaria Notariale:** Investigation. **Giuseppe Corriero:** Writing – review & editing, Supervision, Resources. **Vito Felice Uricchio:** Writing – review & editing, Supervision. **Alessandra Gallo:** Writing – review & editing, Writing – original draft, Supervision, Resources, Methodology, Funding acquisition, Data curation, Conceptualization.

Funding

This research was supported by the Italian Ministry of University and Research (PRIN 2020, Grant N∘ 20204YRYS5 to A.G.). This work was also supported by Portuguese national funds from FCT – Foundation for Science and Technology through projects: **EXPL/CTA-AMB/1613/2021 (DOI: 10.54499/EXPL/CTA-AMB/1613/2021)**; UIDB/04326/2020 (https://doi.org/10.54499/UIDB/04326/2020), UIDP/04326/2020 (https://doi.org/10.54499/UIDP/04326/2020) and LA/P/0101/2020 (https://doi.org/10.54499/LA/P/0101/2020), and from the operational programmes CRESC Algarve 2020 and COMPETE 2020 through project EMBRC.PT ALG-01-0145-FEDER-022121.

Declaration of competing interest

The authors declare that they have no known competing financial interests or personal relationships that could have appeared to influence the work reported in this paper.

Acknowledgements

The authors thank Pasquale Trotti for the morphological analysis of tire particles by Scanning Electron Microscope at the SELGE Lab (Department of Soil, Plant and Food Sciences of the University of Bari Aldo Moro, 70121 Bari, Italy), an Official lab accredited to phytosanitary control according to National regulation art.10 DDMM 14.04.1997 and art. 8 D.M. 09.08.200 – determination Regione Puglia n. 514 12th 11 2013. The authors also wish to acknowledge Mr. Alberto Macina (Rearing of model organisms for the scientific research, Marine Biological Resources service of Stazione Zoologica A. Dohrn) for technical support in mussel maintenance and gamete collection, and Dr. Andrea Sommella for technical assistance in gamete quality assessment.

Appendix A. Supplementary data

Supplementary data to this article can be found online at https://doi.org/10.1016/j.envint.2025.109587.

Data availability

Data will be made available on request.

References

Amaral, A., Lourenço, B., Marques, M., Ramalho-Santos, J., 2013. Mitochondria functionality and sperm quality. Reproduction 146 (5), R163–R174.

Arole, K., Velhal, M., Tajedini, M., Xavier, P.G., Bardasz, E., Green, M.J., Liang, H., 2023. Impacts of particles released from vehicles on environment and health. Tribol. Int., 108417

Bezzaouia, A., Gallo, A., Silvestre, F., Tekaya, S., Tosti, E., 2014. Distribution pattern and activity of mitochondria during oocyte growth and maturation in the ascidian *Styela plicata*. Zygote 22 (4), 462–469.

Boni, R., Gallo, A., Montanino, M., Macina, A., Tosti, E., 2016. Dynamic changes in the sperm quality of *Mytilus galloprovincialis* under continuous thermal stress. Mol. Reprod. Dev. 83 (2), 162–173.

Boni, R., Gallo, A., Tosti, E., 2022. Electrophysiology and fluorescence spectroscopy approaches for evaluating gamete and embryo functionality in animals and humans. Biomolecules 12 (11), 1685.

Capolupo, M., Sørensen, L., Jayasena, K.D.R., Booth, A.M., Fabbri, E., 2020. Chemical composition and ecotoxicity of plastic and car tire rubber leachates to aquatic organisms. Water Res. 169, 115270.

Costa, C.Q., Afonso, I.I., Cruz, J., Teodósio, M.A.A., Jockusch, S., Ramamurthy, V., Power, D.M.D., Silva, J.P., 2024. Environmental markers of plastics and microplastics. Environ. Sci. Technol. 58 (20), 8889–8898.

Degaffe, F.S., Turner, A., 2011. Leaching of zinc from tire wear particles under simulated estuarine conditions. Chemosphere 85 (5), 738–743.

EPA, 1998. Method 6020A (SW-846): Inductively Coupled Plasma-Mass Spectrometry.

Esposito, M.C., Riva, L., Russo, G.L., Punta, C., Corsi, I., Tosti, E., Gallo, A., 2024. Reproductive toxicity assessment of cellulose nanofibers, citric acid, and branched polyethylenimine in sea urchins: Eco-design of nanostructured cellulose sponge framework (Part B). Environ. Pollut. 350, 123934.

Esposito, M.C., Russo, G.L., Riva, L., Punta, C., Corsi, I., Tosti, E., Gallo, A., 2023. Nanostructured cellulose sponge engineered for marine environmental remediation: Eco-safety assessment of its leachate on sea urchin reproduction (Part A). Environ. Pollut. 334, 122169.

Gallo, A., Boni, R., Buttino, I., Tosti, E., 2016. Spermiotoxicity of nickel nanoparticles in the marine invertebrate *Ciona intestinalis* (ascidians). Nanotoxicology 10 (8), 1096–1104.

Gallo, A., Boni, R., Tosti, E., 2018a. Sperm viability assessment in marine invertebrates by fluorescent staining and spectrofluorimetry: a promising tool for assessing marine pollution impact. Ecotoxicol. Environ. Saf. 147, 407–412.

Gallo, A., Esposito, M.C., Boni, R., Tosti, E., 2022. Oocyte quality assessment in marine invertebrates: a novel approach by fluorescence spectroscopy. Biol. Res. 55 (1), 34.

Gallo, A., Esposito, M.C., Tosti, E., Boni, R., 2021. Sperm motility, oxidative status, and mitochondrial activity: Exploring correlation in different species. Antioxidants 10 (7), 1131.

Gallo, A., Manfra, L., Boni, R., Rotini, A., Migliore, L., Tosti, E., 2018b. Cytotoxicity and genotoxicity of CuO nanoparticles in sea urchin spermatozoa through oxidative stress. Environ. Int. 118, 325–333.

Gallo, A., Menezo, Y., Dale, B., Coppola, G., Dattilo, M., Tosti, E., Boni, R., 2018c. Metabolic enhancers supporting 1-carbon cycle affect sperm functionality: an in vitro comparative study. Sci. Rep. 8 (1), 11769.

Gallo, A., Silvestre, F., Cuomo, A., Papoff, F., Tosti, E., 2011. The impact of metals on the reproductive mechanisms of the ascidian *Ciona intestinalis*. Mar. Ecol. 32 (2), 222–231.

Gallo, A., Tosti, E., 2013. Adverse effect of antifouling compounds on the reproductive mechanisms of the ascidian *Ciona intestinalis*. Mar. Drugs 11 (9), 3554–3568.

Gallo, A., Tosti, E., 2015. Reprotoxicity of the antifoulant chlorothalonil in ascidians: an ecological risk assessment. PLoS One 10 (4), e0123074.

Gieré, R., Dietze, V., 2022. Tire-abrasion particles in the environment. In: Gert Heinrich, R.K., Stoček, Radek (Eds.), Degradation of Elastomers in Practice, Experiments and Modeling. Springer, pp. 71–101.

Halsband, C., Sørensen, L., Booth, A.M., Herzke, D., 2020. Car tire crumb rubber: does leaching produce a toxic chemical cocktail in coastal marine systems? Front. Environ. Sci. 8, 557495.

Hua, X., Wang, D., 2023. Tire-rubber related pollutant 6-PPD quinone: a review of its transformation, environmental distribution, bioavailability, and toxicity. J. Hazard. Mater., 132265

Jeong, Y., Lee, S., Woo, S.-H., 2022. Chemical leaching from tire wear particles with various treadwear ratings. Int. J. Environ. Res. Public Health 19 (10), 6006.

Johannessen, C., Helm, P., Lashuk, B., Yargeau, V., Metcalfe, C.D., 2022. The tire wear compounds 6PPD-quinone and 1, 3-diphenylguanidine in an urban watershed. Arch. Environ. Contam. Toxicol. 1–9.

Li, K., Su, H., Xiu, X., Liu, C., Hao, W., 2023. Tire wear particles in different water environments: occurrence, behavior, and biological effects—a review and perspectives. Environ. Sci. Pollut. Res. 30 (39), 90574–90594.

Lian, H., Zhu, L., Zha, C., Li, M., Feng, S., Gao, F., Zhang, X., Xi, Y., Cheng, X., Xiang, X., 2025. Toxicity and intergenerational accumulation effect of tire wear particles and their leachate on *Brachionus plicatilis*. Environ. Pollut. 367, 125635.

Lv, M., Meng, F., Man, M., Lu, S., Ren, S., Yang, X., Wang, Q., Chen, L., Ding, J., 2024. Aging increases the particulate-and leachate-induced toxicity of tire wear particles to microalgae. Water Res. 256, 121653.

O'Loughlin, D.P., Haugen, M.J., Day, J., Brown, A.S., Braysher, E.C., Molden, N., Willis, A.E., MacFarlane, M., Boies, A.M., 2023. Multi-element analysis of tyre rubber for metal tracers. Environ. Int. 178, 108047.

Picard, M., McEwen, B.S., Epel, E.S., Sandi, C., 2018. An energetic view of stress: Focus on mitochondria. Front. Neuroendocrinol. 49, 72–85.

Rackaitis, M., Graves, D., 2017. Rubber. In: James, A., Kent, Tilak, V., Bommaraju, S.D.B. (Eds.), Handbook of Industrial Chemistry and Biotechnology. Springer, pp. 1463–1491.

Reers, M., Smiley, S.T., Mottola-Hartshorn, C., Chen, A., Lin, M., Chen, L.B., 1995. Mitochondrial membrane potential monitored by JC-1 dye. In: Giuseppe, M., Attardi, A.C. (Eds.), Methods in Enzymology. Elsevier, pp. 406–417.

Rist, S., Le Du-Carrée, J., Ugwu, K., Intermite, C., Acosta-Dacal, A., Pérez-Luzardo, O., Zumbado, M., Gómez, M., Almeda, R., 2023. Toxicity of tire particle leachates on early life stages of keystone sea urchin species. Environ. Pollut. 336, 122453.

Romdhani, I., Gallo, A., Venditti, M., Abelouah, M.R., Varchetta, R., Najahi, H., Boukadida, K., Boni, R., Alla, A.A., Minucci, S., 2024a. Unveiling the impact of environmental microplastics on mussel spermatozoa: first evidence of prothymosin-α detection in invertebrate's male gametes. J. Hazard. Mater. 461, 132521.

Romdhani, I., Venditti, M., Gallo, A., Abelouah, M.R., Gaaied, S., Boni, R., Alla, A.A., Minucci, S., Banni, M., 2024b. Environmental microplastics compromise reproduction of the marine invertebrate *Mytilus galloprovincialis:* a holistic approach. J. Hazard. Mater. 480, 136219.

Savino, I., Campanale, C., Trotti, P., Massarelli, C., Corriero, G., Uricchio, V.F., 2022. Effects and impacts of different oxidative digestion treatments on virgin and aged microplastic particles. Polymers 14 (10), 1958.

Senin, M.S., Shahidan, S., Leman, A.S., Hannan, N.I.R.R., 2016. Analysis of physical properties and mineralogical of pyrolysis tires rubber ash compared natural sand in concrete material, 160 (1). IOP Conference Series: Materials Science and Engineering, International Engineering Research and Innovation Symposium (IRIS).

Siddiqui, S., Dickens, J., Cunningham, B., Hutton, S., Pedersen, E., Harper, B., Harper, S., Brander, S., 2022. Internalization, reduced growth, and behavioral effects following exposure to micro and nano tire particles in two estuarine indicator species. Chemosphere 296, 133934.

Stack, M., Hollman, K., Mladenov, N., Harper, B., Pinongcos, F., Sant, K., Rochman, C., Richardot, W., Dodder, N., Hoh, E., 2023. Micron-size tire tread particles leach organic compounds at higher rates than centimeter-size particles: compound identification and profile comparison. Environ. Pollut. 334, 122116.

Tallec, K., Gabriele, M., Paul-Pont, I., Alunno-Bruscia, M., Huvet, A., 2022a. Tire rubber chemicals reduce juvenile oyster (*Crassostrea gigas*) filtration and respiration under experimental conditions. Mar. Pollut. Bull. 181, 113936.

Tallec, K., Huvet, A., Yeuc'h, Le Goïc, V.N., Paul-Pont, I., 2022b. Chemical effects of different types of rubber-based products on early life stages of Pacific oyster, *Crassostrea gigas*. J. Hazard. Mater. 427, 127883.

Turner, A., Rice, L., 2010. Toxicity of tire wear particle leachate to the marine macroalga, *Ulva lactuca*. Environ. Pollut. 158 (12), 3650–3654.

Wagner, S., Hüffer, T., Klöckner, P., Wehrhahn, M., Hofmann, T., Reemtsma, T., 2018. Tire wear particles in the aquatic environment-a review on generation, analysis, occurrence, fate and effects. Water Res. 139, 83–100.

Warnau, M., Temara, A., Jangoux, M., Dubois, P., Iaccarino, M., De Biase, A., Pagano, G., 1996. Spermiotoxicity and embryotoxicity of heavy metals in the echinoid *Paracentrotus lividus*. Environ. Toxicol. Chem. 15 (11), 1931–1936.

Wik, A., Dave, G., 2009. Occurrence and effects of tire wear particles in the environment–a critical review and an initial risk assessment. Environ. Pollut. 157 (1), 1–11.

Xaydarali, F., 2022. Analysis of the chemical composition of car tire rubber. Int. J. Adv. Sci. Res. 2 (12), 183–191.

Yang, K., Jing, S., Liu, Y., Zhou, H., Liu, Y., Yan, M., Yi, X., Liu, R., 2022. Acute toxicity of tire wear particles, leachates and toxicity identification evaluation of leachates to the marine copepod *Tigriopus japonicus*. Chemosphere 297, 134099.

Yang, K., You, K., Liu, Y., Zhou, H., Zhan, J., Cheng, H., Yi, X., 2025. Effects of long-term exposure to tire wear particle leachate on life-cycle chronic toxicity and potential toxic mechanisms in the marine copepod *Tigriopus japonicus*. Water Res. 123384.

Zhang, H.-Y., Huang, Z., Liu, Y.-H., Hu, L.-X., He, L.-Y., Liu, Y.-S., Zhao, J.-L., Ying, G.-G., 2023. Occurrence and risks of 23 tire additives and their transformation products in an urban water system. Environ. Int. 171, 107715.